Onset of the Efficiency Droop in GaInN Quantum Well Light-Emitting Diodes under Photoluminescence and Electroluminescence Excitation

ARTICLE · JULY 2015

DOI: 10.1021/acsphotonics.5b00305

5 AUTHORS, INCLUDING:

Guan-Bo Lin

Rensselaer Polytechnic Institute

20 PUBLICATIONS **197** CITATIONS

SEE PROFILE

Ef Schubert

Rensselaer Polytechnic Institute

155 PUBLICATIONS **5,611** CITATIONS

SEE PROFILE

Jaehee Cho

Chonbuk National University

124 PUBLICATIONS **2,124** CITATIONS

SEE PROFILE

Jong Kyu Kim

Pohang University of Science and Technology

190 PUBLICATIONS **6,616** CITATIONS

SEE PROFILE

ACS Photonics

Letter

pubs.acs.org/journal/apchd5

Onset of the Efficiency Droop in GaInN Quantum Well Light-Emitting Diodes under Photoluminescence and Electroluminescence Excitation

Guan-Bo Lin,[*,†] E. Fred Schubert,[†] Jaehee Cho,[*,‡] Jun Hyuk Park,[§] and Jong Kyu Kim[§]

[†]Department for Electrical, Computer, and Systems Engineering, Rensselaer Polytechnic Institute, Troy, New York 12180, United States

[‡]School of Semiconductor and Chemical Engineering, Semiconductor Physics Research Center, Chonbuk National University, Jeonju 561-756, Republic of Korea

[§]Department of Materials Science and Engineering, Pohang University of Science and Technology (POSTECH), Pohang, Gyeongbuk 790-784, Republic of Korea

ABSTRACT: The efficiency of $Ga_{0.87}In_{0.13}N$/GaN single and multiple quantum well (QW) light-emitting diodes is investigated under photoluminescence (PL) and electroluminescence (EL) excitation. By measuring the laser spot area (knife-edge method) and the absorbance of the GaInN QW (transmittance/reflectance measurements), the PL excitation density can be converted to an equivalent EL excitation density. The EL efficiency droop-onset occurs at an excitation density of 2.08×10^{26} cm^{-3} s^{-1} (J = 10 A/cm^2), whereas no PL efficiency droop is found for excitation densities as high as 3.11×10^{27} cm^{-3} s^{-1} (J = 149 A/cm^2). Considering Shockley–Read–Hall, radiative, and Auger recombination and including carrier leakage shows that the EL efficiency droop is consistent with a reduction of injection efficiency.

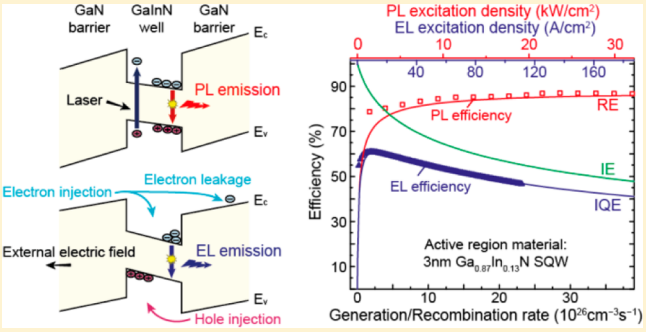

KEYWORDS: *light-emitting diode, efficiency droop, nitride semiconductor, solid-state lighting*

III-Nitride-based light-emitting diodes (LEDs) are next-generation lighting sources because of their high luminous efficiency, compact size, and strong durability. However, one material-related difficulty, i.e., the efficiency droop, exists in all III-nitride-based LEDs and has not yet been solved.[1] The efficiency droop is the phenomenon where the internal quantum efficiency (IQE) gradually declines with increasing current density after reaching a peak efficiency at a relatively small current density, usually between 1 and 10 A/cm^2. The droop phenomenon has also been found in photoluminescence (PL) measurements.[2] The efficiency droop issue hinders LEDs from reaching their optimal efficiency performance and introduces problems when pursuing high-brightness applications.

The cause of the efficiency droop is still under debate. Suspected causes such as Auger recombination,[3,4] carrier delocalization,[5,6] and carrier leakage[7,8] have been published in recent years. To identify the true cause, the droop found in PL is usually compared with the droop found in electroluminescence (EL). In PL experiments, if the wavelength of the laser excitation source is appropriately chosen (i.e., by using below-GaN-band-gap excitation), carriers are exclusively generated in and confined to the blue-emitting GaInN quantum wells (QWs), and thus all carrier recombination occurs exclusively inside the active region. In contrast to PL experiments, carrier recombination both inside and outside the active region is possible when injecting carriers during EL experiments.

Several previous studies concerned the temperature dependence of recombination pathways for both the radiative and nonradiative components.[6−8,11,14−16] Furthermore, several previous studies have shown that the excitation density at the onset of the PL droop coincides with that at the onset of the EL droop, and thus the EL and PL droop are likely caused by the same nonradiative recombination inside the active region.[2,9] However, there are also reports that found little or no efficiency droop at optical excitation densities of kW/cm^2 in PL measurements.[1,10] Furthermore, several other mechanisms, such as carrier delocalization,[11] carrier heating,[12] and stimulated emission,[13] have also been reported to cause the PL efficiency droop. The reported droop-onset PL excitation densities (incident densities) are usually on the order of MW/cm^2. The conversion of PL excitation density to an equivalent current density will help in resolving the question of whether the mechanism causing the PL droop is identical to that causing

Received: June 2, 2015
Published: July 29, 2015

DOI: 10.1021/acsphotonics.5b00305
ACS Photonics 2015, 2, 1013−1018

the EL droop. In this report, a detailed experimental investigation is conducted to clarify if the efficiency droops under EL and PL excitation are phenomena caused by the same physical mechanism.

METHODS

Three different samples grown by metal−organic vapor-phase epitaxy are prepared. They are the single QW pn-junction LED ("SQW LED"), the five multiple QW LED ("5QW LED"), and the n-type GaN/SQW/n-type GaN sample ("n/SQW/n sample"). A detailed description of the SQW LED and the n/SQW/n sample can be found in a previous report.[14] Before stating our main experiment and results, we note that the samples used in this study have an adequate quality for investigating the typical phenomenon of PL and EL droop.

Power-dependent PL is implemented to characterize the LEDs as well as unipolar n/SQW/n sample structures. A high-power 405 nm GaInN injection laser diode is driven by a power supply and modulated by an Agilent 8114A pulse generator. The laser spectrum and beam shape are optimized by a band-pass filter and an optical iris, respectively. The laser beam is focused on the sample stage, and the incident laser power is measured by a photodetector connected to a power meter. The blue PL from the sample is collimated, filtered by a long-wavelength pass filter (cutoff 420 nm), and collected by a spectrometer. The PL spectral power is integrated over wavelength so that the PL intensity is obtained. By means of optical goniometry, we have verified that the far-field pattern of the PL and EL emission does not depend on the excitation strength so that integrating-sphere measurements are not necessary and would be redundant. Next, we examine the (i) modulation of the laser power, (ii) laser spot size, and (iii) absorbance of a GaInN QW.

The PL excitation wavelength (405 nm) is chosen to selectively excite free carriers in the blue-emitting GaInN QWs. The excitation wavelength is longer than GaN band-gap luminescence ($\lambda_{GaN} \approx 361$ nm). Given that carrier leakage out of the QWs in the high-excitation limit during photoexcitation can be neglected,[18] and given that the n/SQW/n sample has no pn-junction built-in electric field, a unity injection efficiency (IE = 1.0) can be assumed for PL measurements.

First, a linear relationship between electrical input voltage and laser output power is confirmed by using an optical power meter, ensuring that the laser power can be tuned linearly by an external power supply (in the range 3.5 to 11.0 V). The laser is pulsed with a 1% duty cycle, and the photodiode (PD)-measured average power (P_{PD}) ranges from 0.135 to 2.91 mW; that is, the laser power P_{laser} is linear in the range 13.5 to 291 mW. The laser pulse can be precisely controlled by the pulse generator, as confirmed by the laser output (measured by the photodetector) having the same square waveform as the pulse generator input.

Second, the laser spot size on the sample is determined by the knife-edge method. An opaque razor blade is positioned on the sample stage with the laser irradiating downward (z-direction) on the blade. When moving the blade in one horizontal direction (x- or y-direction), the blade initially blocks the laser beam and then gradually decreases the level of blockage. This process allows us to measure the spatial laser beam profile. The blade movement is controlled by micrometer adjustment. On the basis of the positions measured at 5% and 95% of peak laser power, we determine the 5/95 diameter of the laser spot. We find that the spot is elliptical, as is common in the far-field pattern of semiconductor lasers. Assuming that the laser profile follows the Gaussian distribution, the measured laser power is the integral of the Gaussian function, i.e., the error function. In Figure 1, the measured laser power (black squares) is fitted by the error function (red line), and the Gaussian power profile is extracted (blue line). The major and minor diameter of the ellipse is 73.4 and 13.9 μm, respectively. Therefore, 90% of the incident power is enclosed in the laser spot area A_{spot} (8.01×10^{-6} cm^2). The laser spot area does not change significantly when the laser power changes.

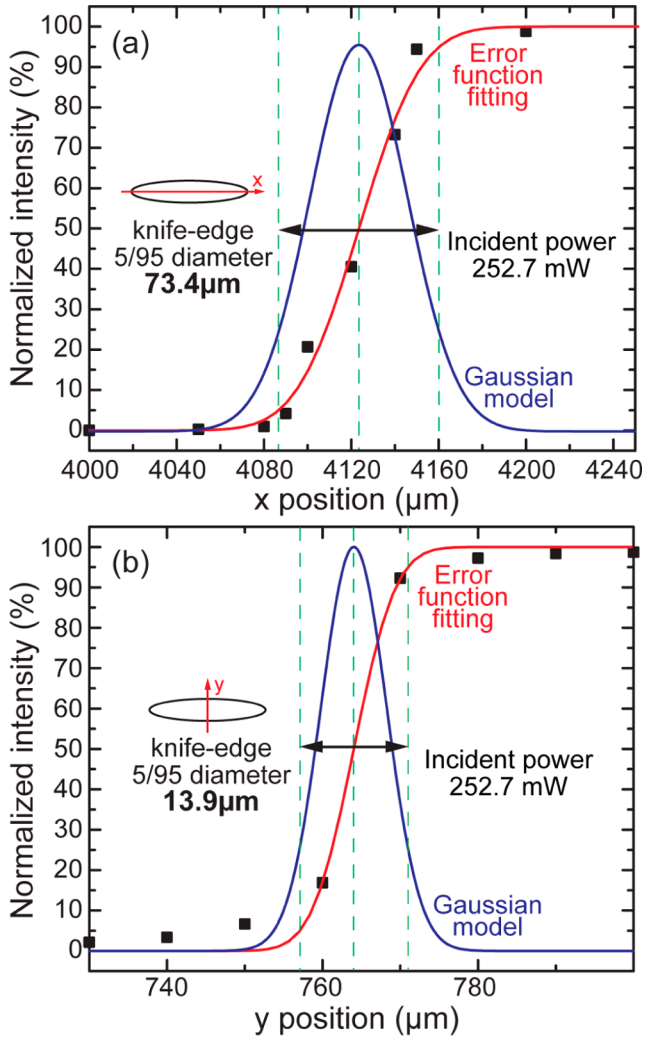

Figure 1. Measured laser intensity (black squares) and the error-function fitting (red line) vs blade position in the (a) x- and (b) y-direction. The Gaussian profile (blue line) is the derivative of the fitted error function. The three vertical green dashed lines cross at 5%, 50%, and 95% of the normalized intensity. The 5/95 diameter in the x- and y-direction is 73.4 and 13.9 μm, respectively.

Third and last, transmittance/reflectance experiments are conducted to measure the absorbance of the $Ga_{0.87}In_{0.13}N$ QW sample (λ = 440 nm), and the result is compared with the theoretical value[15] and other reported results.[16] In our PL setup, the 405 nm laser source excites only GaInN QWs but not GaN material (resonant excitation). A 5QW GaInN/GaN LED grown on a back-side-polished sapphire substrate (so that optical scattering can be neglected) is placed in a JASCO spectrophotometer to measure the reflectance and trans-

DOI: 10.1021/acsphotonics.5b00305
ACS Photonics 2015, 2, 1013−1018

mittance. As a result, the summation of reflectance, absorbance, and transmittance yields the unit value (1.0). In Figure 2a, the

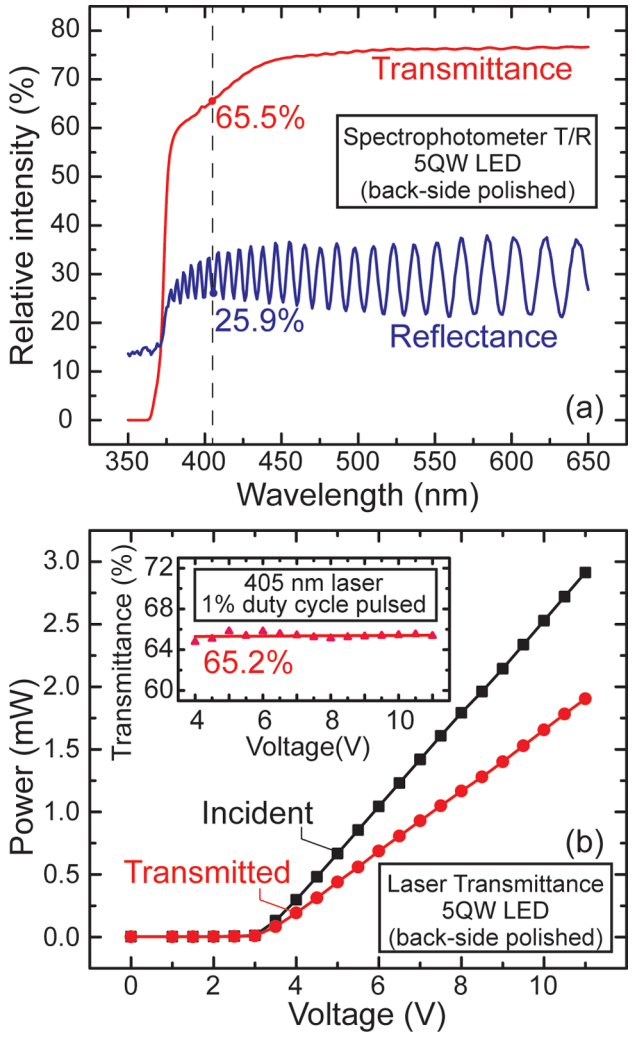

Figure 2. (a) Optical transmittance and reflectance of 5QW LED grown on a back-side-polished sapphire substrate; 65.5% transmittance and 25.9% reflectance are measured at 405 nm. (b) Incident and transmitted laser power vs laser driving voltage; 65.2% transmittance is measured at 405 nm.

measured reflectance and transmittance of the 5QW GaInN/GaN LED at the wavelength of 405 nm is 25.9% and 65.5%, respectively. Note that the 405 nm wavelength is dictated by the GaInN injection laser that we use as excitation source. Consequently, the absorbance of 5 GaInN QWs is 8.6% and the absorbance per QW is 1.7%. This absorbance is similar to that of GaInN blue-emitting QWs reported in the literature.[16] The theoretical absorption coefficient of $Ga_{0.87}In_{0.13}N$ at 405 nm is 6.67×10^4 cm^{-1}, as calculated from the simplified van Roosbroeck–Shockley equation.[15,17] Therefore, the calculated absorbance of a 3 nm $Ga_{0.87}In_{0.13}N$ QW at 405 nm is 2.0%, similar to the measured value.

In Figure 2b, power-dependent PL is conducted to rule out absorption saturation in the GaInN QW, which is examined by measuring the transmittance for increasing laser power. We find a constant transmittance. Since reflectance is related only to the refractive index of the sample's top layer (GaN), it is constant as well. Therefore, the absorbance is constant for all excitation densities used in the PL measurements.

Using the above information, the incident PL excitation density (measured in kW/cm^2) can be converted to an (optical) generation rate (cm^{-3} s^{-1}). Likewise, the EL excitation density (A/cm^2) can be converted to an (electrical) generation rate (cm^{-3} s^{-1}). This allows for the conversion of the incident PL excitation density to an equivalent EL excitation density. The PL generation rate (G_{PL}) is given by

$$G_{PL} = \frac{P_{laser} f_{in} A}{A_{spot} h\nu d_{QW}} \quad (1)$$

where $h\nu$ is the 405 nm photon energy, A is the absorbance per QW with a thickness of d_{QW}, and f_{in} is the fraction of the laser power within A_{spot}. For example, a laser power of P_{laser} = 176 mW ($A_{spot} = 8.01 \times 10^{-6}$ cm^2; $h\nu$ = 3.06 eV; f_{in} = 90%) incident on a single QW (d_{QW} = 3 nm; A = 1.7%) gives an incident laser power density of 19.8 kW/cm^2 and a PL generation rate (G_{PL}) of 22.9×10^{26} cm^{-3} s^{-1}. Furthermore, the EL generation rate, G_{EL}, is given by

$$G_{EL} = \frac{J}{e d_{QW}} \quad (2)$$

where J, e, and d_{QW} are the current density, elementary charge, and thickness of the QW (active region), respectively. For example, a current density of 110 A/cm^2 corresponds to an equivalent EL generation rate (G_{EL}) of 22.9×10^{26} cm^{-3} s^{-1} and an equivalent PL incident excitation density of 19.8 kW/cm^2.

Next, the PL and EL efficiency behavior is compared for the SQW LED and the 5QW LED. The EL measurement is conducted using an Agilent 4155C semiconductor parameter analyzer. The input current is pulsed at 1% duty cycle with 1 ms pulse duration to avoid heating effects. The EL intensity is collected by a photodiode. The PL intensity is integrated from the spectral power density measured by a spectrometer. In addition, the SQW LED and the n-type/SQW/n-type (n/SQW/n) sample are measured in PL. At low PL excitation density, carrier leakage from the QW active region of LEDs has been shown to occur;[18] on the other hand, at high PL excitation densities, self-biasing due to the leaked carriers leads to strong carrier confinement.[18] We note that, in contrast to the SQW LED, the n/SQW/n sample, because it does not exhibit carrier leakage at low PL excitation density, can be appropriately modeled by the *ABC* model.

RESULTS AND DISCUSSION

The measured efficiency vs excitation density curves of the SQW LED and 5QW LED are plotted in Figure 3. Inspection of the figure reveals that for the SQW LED the onset of the EL efficiency droop is pronounced and occurs at an injection rate of 2.08×10^{26} cm^{-3} s^{-1}. In contrast, no significant droop is observed in PL up to an excitation rate of 35.0×10^{26} cm^{-3} s^{-1}. The PL and EL efficiency show a pronounced disparity in both the magnitude of the droop and the onset excitation density. A similar disparity is found in the 5QW LED, in which the onset of EL droop occurs at 1.39×10^{26} cm^{-3} s^{-1}, while no significant PL droop is found up to 35.0×10^{26} cm^{-3} s^{-1}.

That is, EL exhibits a strong droop at a relatively low excitation density, whereas PL exhibits no significant droop even for 15-times-higher excitation density. This disparity suggests that the mechanism causing EL efficiency droop is

DOI: 10.1021/acsphotonics.5b00305
ACS Photonics 2015, 2, 1013–1018

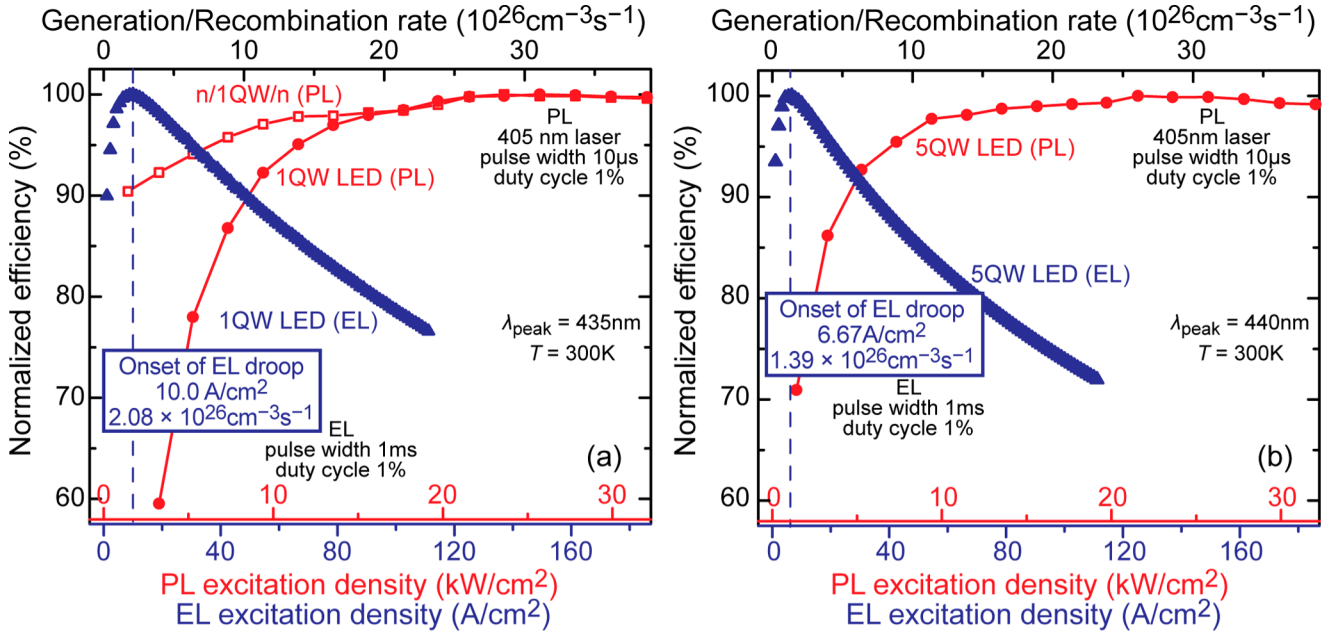

Figure 3. (a) Efficiency vs excitation density curves of an n/SQW/n sample excited by PL and a SQW LED excited by both PL and EL. (b) Efficiency vs excitation density curves of a SQW LED sample excited by both PL and EL.

different and stronger than the mechanism causing the PL efficiency droop. At room temperature, the PL behavior of a blue-emitting GaInN QW does not display droop in the efficiency for excitation densities as high as 30 kW/cm^2, consistent with reported PL results.[1,2]

Next, we investigate the dependence of the efficiency on carrier density. At the onset point of the droop (i.e., the maximum-efficiency point), there is general agreement that (i) the injection efficiency is close to unity (IE ≈ 1.0) and (ii) radiative recombination is the dominant recombination channel. In the droop regime, the injection efficiency may decrease due to a lack of hole injection (causing the droop). To better understand the difference between PL and EL efficiency behavior, we employ the drift-leakage model[8] to investigate the loss mechanism at high excitation density under both EL and PL excitation. For PL excitation in an n/SQW/n sample (no built-in field), carriers are confined to the active region so that carrier-leakage becomes negligible. In the steady state, the PL generation rate G_{PL} and the recombination rate can be adequately described by the equation

$$G_{PL} = A_{SRH}n + Bn^2 \tag{3}$$

where A_{SRH}, B, and n are the Shockley–Read–Hall, radiative, and the optically generated carrier concentration, respectively. In the experimental PL efficiency curve, the PL efficiency droop is not significant up to 30 kW/cm^2 in optical excitation density. This result is similar to the finding of a PL efficiency plateau reported in the literature.[10] Therefore, using the first two recombination terms of the ABC model (i.e., $A_{SRH}n + Bn^2$) is mathematically sufficient to describe the experimental PL efficiency. That is, Auger recombination is negligible for generation rates lower than 10^{27} cm^{-3} s^{-1}.

The IQE is defined as the product of injection efficiency, IE, and radiative efficiency (RE). In the n/SQW/n sample under photoexcitation, we can safely assume that IE = 1.

$$\mathrm{IQE} = \mathrm{IE} \times \mathrm{RE} = 1 \times \frac{Bn^2}{G_{PL}} \tag{4}$$

Solving this equation for the carrier concentration n yields

$$n = \sqrt{\frac{\mathrm{IQE} \times G_{PL}}{B}} = \sqrt{\frac{\mathrm{RE}_{peak}}{B}}\sqrt{G_{PL} \times \mathrm{EQE}_{n,PL}} \tag{5}$$

where RE_{peak} is the peak radiative efficiency determined to be 87%,[14] and the $\mathrm{EQE}_{n,PL}$ is the normalized efficiency in PL. Since the reported radiative coefficient B of GaInN material is commonly believed to be between 10^{-11} and 10^{-10} cm^3 s^{-1}, we assume $B = 5.0 \times 10^{-11}$ cm^3 s^{-1} and obtain $A_{SRH} = 3.18 \times 10^7$ s^{-1} by fitting eq 3 to the experimental G_{PL} vs n curve. The goodness-of-fit is excellent no matter what radiative coefficient B is chosen (in the range 10^{-11} and 10^{-10} cm^3 s^{-1}).

Next, we describe the EL generation rate fitting for EL measurements. In EL measurements, in addition to the original ABC recombination channels, carrier leakage must be considered. Assuming the drift-leakage (DL) mechanism, which obeys cubic dependence on the carrier concentration, we write EL generation rate, G_{EL},

$$G_{EL} = A_{SRH}n + Bn^2 + C_{DL}n^3 \tag{6}$$

In the EL case, IE is not a unit value, and IQE is

$$\mathrm{IQE} = \mathrm{IE} \times \mathrm{RE} = \frac{G_{PL}}{G_{EL}}\frac{Bn^2}{G_{PL}} \tag{7}$$

Solving this equation for the carrier concentration yields

$$n = \sqrt{\frac{\mathrm{IQE} \times G_{EL}}{B}} = \sqrt{\frac{\mathrm{IQE}_{peak}}{B}}\sqrt{G_{EL} \times \mathrm{EQE}_{n,EL}} \tag{8}$$

We estimate that IQE_{peak} ranges between 50% and 85%, and we choose 5% steps consistent with reported IQE for blue LEDs.[19−21] Using these values results in different carrier concentrations (see eq 8) and different goodness-of-fit. By judging from the goodness-of-fit, the most suitable IQE_{peak} can

DOI: 10.1021/acsphotonics.5b00305
ACS Photonics 2015, 2, 1013−1018

be determined. When performing the EL fitting, we use the same A_{SRH} and B parameters obtained from the PL fitting since the crystal quality of GaInN QW is the same. The optimal IQE_{peak} is 60% for the SQW LED measured in EL experiments, and the extracted leakage coefficient (C_{DL}) is 5.86×10^{-30} cm^6 s^{-1}.

By using all fitted coefficients (A_{SRH}, B, and C_{DL}), the model curve of IQE, IE, and RE vs generation rate can be derived from eq 7. The model curves as well as the experimental PL and EL efficiency for the active material, for a 3 nm $Ga_{0.87}In_{0.13}N$ single QW, are plotted in Figure 4. Inspection of the figure reveals that the model can fully explain the experimental differences between PL and EL efficiency behavior.

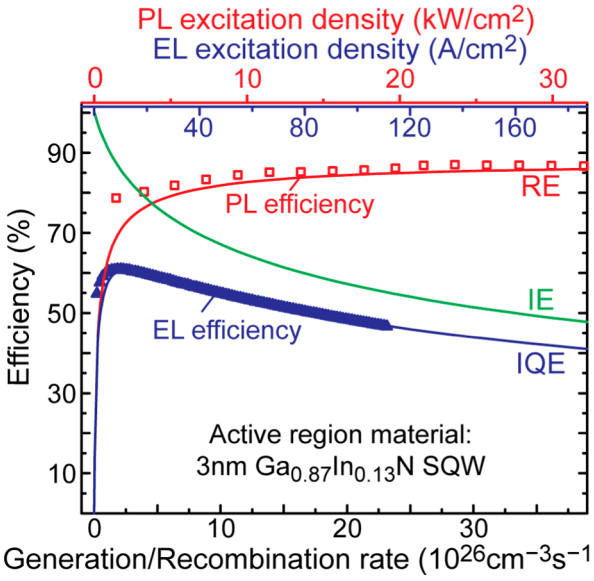

Figure 4. Measured EL and PL efficiency (300 K) and modeled curves of IQE, IE, and RE for a 3 nm Ga0.87In0.13N/GaN SQW structure.

Although the simple theoretical model used here allows one to determine the carrier density at the onset point of the droop (i.e., the maximum-efficiency point), the abscissa axes of Figure 4 depict the "generation/recombination rate" because these values are derived directly from the experimental results and thus are not subject to a potential uncertainty in the simple theoretical model. We are grateful for a comment by a referee of the present paper who points out that advanced microscopic theory including many-body effects may yield more accurate values with respect to the carrier densities, e.g., at the onset point of the droop.

CONCLUSION

A careful determination of the laser spot area and the absorbance of a $Ga_{0.87}In_{0.13}N$ QW is made. This determination allows for the conversion between PL excitation density and EL excitation density and a comparison between PL and EL efficiency. The PL efficiency droop is not significant at a generation rate of 35×10^{26} cm^{-3} s^{-1}, which is 15 times higher than the onset excitation density of EL efficiency droop for the same active-region material (3 nm $Ga_{0.87}In_{0.13}N$ SQW). PL experiments show that the loss mechanism inside the active material is not strong enough to cause PL efficiency droop for an equivalent EL excitation range of up to 160 A/cm^2. By incorporating the carrier leakage model into the *ABC* model, comprehensive information on recombination parameters is obtained including the A_{SRH} (3.18×10^7 s^{-1}), B (5.0×10^{-11} cm^3 s^{-1}) and C_{DL} (5.86×10^{-30} cm^6 s^{-1}) coefficients, the IQE_{peak} (60%), and the efficiency vs generation rate model curves. Electron leakage explains the EL efficiency droop, indicating that the Auger recombination is negligible for the EL excitation range employed.

AUTHOR INFORMATION

Corresponding Authors

*E-mail (G.-B. Lin): ling4@rpi.edu.

*E-mail (J. Cho): jcho@chonbuk.ac.kr.

Author Contributions

The manuscript was written through contributions of all authors. All authors have given approval to the final version of the manuscript.

Notes

The authors declare no competing financial interest.

ACKNOWLEDGMENTS

The authors gratefully acknowledge support by Samsung Electronics, Sandia National Laboratories, the U.S. National Science Foundation, and Korea Institute for Advancement of Technology. G.-B.L. and E.F.S. were supported by Sandia's Solid-State Lighting Sciences Center, an Energy Frontier Research Center funded by the U.S. Department of Energy, Office of Basic Energy Sciences. J.C. acknowledges the support by the Basic Science Research Program through the National Research Foundation (NRF) of Korea funded by the Ministry of Education (2014R1A1A2054092).

REFERENCES

(1) Kim, M. H.; Schubert, M. F.; Dai, Q.; Kim, J. K.; Schubert, E. F.; Piprek, J.; Park, Y. Origin of efficiency droop in GaN-based light-emitting diodes. *Appl. Phys. Lett.* **2007**, *91*, 183507.

(2) Laubsch, A.; Sabathil, M.; Bergbauer, W.; Strassburg, M.; Lugauer, H.; Peter, M.; Lutgen, S.; Linder, N.; Streubel, K.; Hader, J. On the origin of IQE-'droop' in InGaN LEDs. *Phys. Status Solidi C* **2009**, *6*, S913.

(3) Kioupakis, E.; Rinke, P.; Delaney, K. T.; Van de Walle, C. G. Indirect Auger recombination as a cause of efficiency droop in nitride light-emitting diodes. *Appl. Phys. Lett.* **2011**, *98*, 161107.

(4) Iveland, J.; Martinelli, L.; Peretti, J.; Speck, J. S.; Weisbuch, C. Direct Measurement of Auger Electrons Emitted from a Semiconductor Light-Emitting Diode under Electrical Injection: Identification of the Dominant Mechanism for Efficiency Droop. *Phys. Rev. Lett.* **2013**, *110*, 177406.

(5) Hammersley, S.; Watson-Parris, D.; Dawson, P.; Godfrey, M.; Badcock, T.; Kappers, M.; McAleese, C.; Oliver, R.; Humphreys, C. The consequences of high injected carrier densities on carrier localization and efficiency droop in InGaN/GaN quantum well structures. *J. Appl. Phys.* **2012**, *111*, 083512.

(6) Badcock, T. J.; Hammersley, S.; Watson-Parris, D.; Dawson, P.; Godfrey, M. J.; Kappers, M. J.; McAleese, C.; Oliver, R. A.; Humphreys, C. J. Carrier Density Dependent Localization and Consequences for Efficiency Droop in InGaN/GaN Quantum Well Structures. *Jpn. J. Appl. Phys.* **2013**, *52*, 08JK10.

(7) Meyaard, D. S.; Lin, G.-B.; Cho, J.; Schubert, E. F.; Shim, H. W.; Han, S. H.; Kim, M. H.; Sone, C.; Kim, Y. S. Identifying the cause of the efficiency droop in GaInN light-emitting diodes by correlating the onset of high injection with the onset of the efficiency droop. *Appl. Phys. Lett.* **2013**, *102*, 251114.

(8) Lin, G.-B.; Meyaard, D. S.; Cho, J.; Schubert, E. F.; Shim, H. W.; Sone, C. Analytic model for the efficiency droop in semiconductors

DOI: 10.1021/acsphotonics.5b00305
ACS Photonics 2015, 2, 1013−1018

with asymmetric carrier-transport properties based on drift-induced reduction of injection efficiency. *Appl. Phys. Lett.* **2012**, *100*, 161106.
(9) Shen, Y. C.; Mueller, G. O.; Watanabe, S.; Gardner, N. F.; Munkholm, A.; Krames, M. R. Auger recombination in InGaN measured by photoluminescence. *Appl. Phys. Lett.* **2007**, *91*, 141101.
(10) Xie, J.; Ni, X.; Fan, Q.; Shimada, R.; Özgür, Ü.; Morkoç, H. On the efficiency droop in InGaN multiple quantum well blue light emitting diodes and its reduction with p -doped quantum well barriers. *Appl. Phys. Lett.* **2008**, *93*, 121107.
(11) Mickevičius, J.; Tamulaitis, G.; Shur, M.; Shatalov, M.; Yang, J.; Gaska, R. Correlation between carrier localization and efficiency droop in AlGaN epilayers. *Appl. Phys. Lett.* **2013**, *103*, 011906.
(12) Tamulaitis, G.; Mickevičius, J.; Dobrovolskas, D.; Kuokštis, E.; Shur, M. S.; Shatalov, M.; Yang, J.; Gaska, R. Carrier dynamics and efficiency droop in AlGaN epilayers with different Al content. *Phys. Status Solidi C* **2012**, *9*, 1677.
(13) Mickevičius, J.; Jurkevičius, J.; Shur, M. S.; Yang, J.; Gaska, R.; Tamulaitis, G. Photoluminescence efficiency droop and stimulated recombination in GaN epilayers. *Opt. Express* **2012**, *20* (23), 25195.
(14) Lin, G.-B.; Shan, Q.; Birkel, A. J.; Cho, J.; Schubert, E. F.; Crawford, M. H.; Westlake, K. R.; Koleske, D. D. Method for determining the radiative efficiency of GaInN quantum wells based on the width of efficiency-versus-carrier-concentration curve. *Appl. Phys. Lett.* **2012**, *101*, 241104.
(15) Dai, Q.; Schubert, M. F.; Kim, M. H.; Kim, J. K.; Schubert, E. F.; Koleske, D. D.; Crawford, M. H.; Lee, S. R.; Fischer, A. J.; Thaler, G.; Banas, M. A. Internal quantum efficiency and nonradiative recombination coefficient of GaInN/GaN multiple quantum wells with different dislocation densities. *Appl. Phys. Lett.* **2009**, *94*, 111109.
(16) Song, J.-H.; Kim, H.-J.; Ahn, B.-J.; Dong, Y.; Hong, S.; Song, J.-H.; Moon, Y.; Yuh, H.-K.; Choi, S.-C.; Shee, S. Role of photovoltaic effects on characterizing emission properties of InGaN/GaN light emitting diodes. *Appl. Phys. Lett.* **2009**, *95*, 263503.
(17) Schubert, E. F. *Light-Emitting Diodes*, 2nd ed.; Cambridge University Press: The Edinburgh Building, 2006.
(18) Schubert, M. F.; Dai, Q.; Xu, J.; Kim, J. K.; Schubert, E. F. Electroluminescence induced by photoluminescence excitation in GaInN/GaN light-emitting diodes. *Appl. Phys. Lett.* **2009**, *95*, 191105.
(19) Wierer, J. J.; David, A.; Megens, M. M. III-nitride photonic-crystal light-emitting diodes with high extraction efficiency. *Nat. Photonics* **2009**, *3*, 163−169.
(20) Pimputkar, S.; Speck, J. S.; DenBaars, S. P.; Nakamura, S. Prospects for LED lighting. *Nat. Photonics* **2009**, *3*, 180−182.
(21) Laubsch, A.; Sabathil, M.; Baur, J.; Peter, M.; Hahn, B. High-Power and High-Efficiency InGaN-Based Light Emitters. *IEEE Trans. Electron Devices* **2010**, *57* (1), 79−87.

DOI: 10.1021/acsphotonics.5b00305
ACS Photonics 2015, 2, 1013−1018